

## Compact Zoom Lens Design for a 5x Mobile Camera Using Prism

Sung-Chan Park\* and Sang-Hun Lee

*Department of Physics, Dankook University, Cheonan 330-714, Korea*

Jong-Gyu Kim

*Department of Chemistry, Dankook University, Cheonan 330-714, Korea*

(Received April 6, 2009 : accepted April 15, 2009)

This study presents the compact zoom lens with a zoom ratio of 5x for a mobile camera by using a prism. The lens modules and aberrations are applied to the initial design for a four-group inner-focus zoom system. An initial design with a focal length range of 4.4 to 22.0 mm is derived by assigning the first-order quantities and third-order aberrations to each module along with the constraints required for optimum solutions. We separately designed a real lens for each group and then combined them to establish an actual zoom system. The combination of the separately designed groups results in a system that satisfies the basic properties of the zoom system consisting of the original lens modules. In order to have a slim system, we directly inserted the right-angle prism in front of the first group. This configuration resulted in a more compact zoom system with a depth of 8 mm. The finally designed zoom lens has an f-number of 3.5 to 4.5 and is expected to fulfill the requirements for a slim mobile zoom camera having high zoom ratio of 5x.

*Keywords* : Mobile camera, Lens modules, Zoom lens design, Aberrations

*OCIS codes* : (220.0220) Optical design and fabrication; (120.3620) Lens design; (230.0230) Optical devices

### I. INTRODUCTION

A zoom system is a mechanical assembly of lens elements with the ability to vary its focal length, by moving the sub-groups along the axis. It is commonly used to take a picture or motion images. Zoom systems have been developed over past decades for different purposes. The most common zoom system is a multiple conjugates system allowing objects to be imaged on a CCD image sensor with different scales. Designing a zoom lens consists of finding out the coupled motions of lens elements to accomplish the continuous variations of magnification or focal length. During the zooming, only the separations between elements vary at each zoom position. These separations are designated as an adjustment for changing magnifications and maintaining the image in focus.

Initial design methods for zoom lens are usually divided into two ways. One is the paraxial analysis based on

thin lens theory, the other is the optimized solution from lens modules design. The paraxial analysis has several disadvantages. It is difficult to judge if the solutions satisfy all the requirements for the zoom system [1-3]. In contrast to the paraxial method, since the lens module method employed in this study involves lots of physical quantities of the optical system, the first-order and third-order aberrations can be manipulated directly by using lens modules. Several lenses have been designed and evaluated by lens modules [4-5].

In this paper, lens modules and aberration theory are used to discuss the optimum initial design of a 5x, four-group inner-focus zoom system. This initial zoom system is designed to satisfy specific requirements, and the real lens designs are obtained from the lens modules by using an automatic design method. After balancing of the higher-order aberrations, we obtained the zoom system that has the aperture of F/3.5 at position 1 to F/4.5 at position 3 and zoom ratio of 5x.

---

\*Corresponding author: scpark@dankook.ac.kr

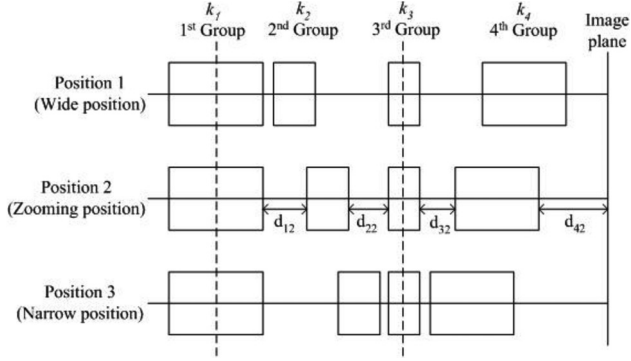


FIG. 1. Schematic diagram of the four-group inner-focus zoom lens.

## II. INITIAL ZOOM LENS DESIGN

Figure 1 illustrates the four-group inner-focus zoom system. From the object to the image side, the zoom system is composed of a fixed front group, a second lens group for zooming, a fixed third lens group, and a fourth lens group for focusing. Their powers are denoted  $K_1$ ,  $K_2$ ,  $K_3$ , and  $K_4$ , respectively. The first and the third groups are always fixed. While second group moves to the right to have a longer focal length, the fourth group should move to keep the image position stationary.

When the displacement of the groups for zooming is zero, *i.e.*, at position 1, the focal length of zoom lens is the shortest, so that it is the wide-field position. Meanwhile, the displacement of the second lens group is the maximum at position 3, and the zoom system has its longest focal length at this position. Therefore, it is called the narrow-field position. The position 2 is located halfway between position 1 and position 3. The distances between the preceding group and the succeeding group are denoted by  $d_{j2}$  ( $j=1, 2, 3, 4$ ) at position 2.

Each group is generally composed of several thick lens elements. When the higher-order aberrations are neglected, the properties of the lens system can be specified by its first-order quantities and the third-order wave aberrations at given conjugate points [6]. In other words, if the first-order quantities and the third-order aberrations of the lens module are assigned to the real lens group, then both lens systems are equivalent to each other to within the limit of the first- and the third-order properties. Hence, each group of the zoom system can be replaced by its thick lens module by specifying its focal length ( $FL_M$ ), front focal length ( $FF_M$ ), back focal length ( $BF_M$ ), magnification ( $MG_M$ ), entrance pupil position ( $EP_M$ ), entrance pupil diameter ( $ED_M$ ), field angle ( $\beta$ ), and third-order aberrations [7-9].

We have set up the zoom lens system shown in Fig. 1 with four thick-lens modules, for which initial

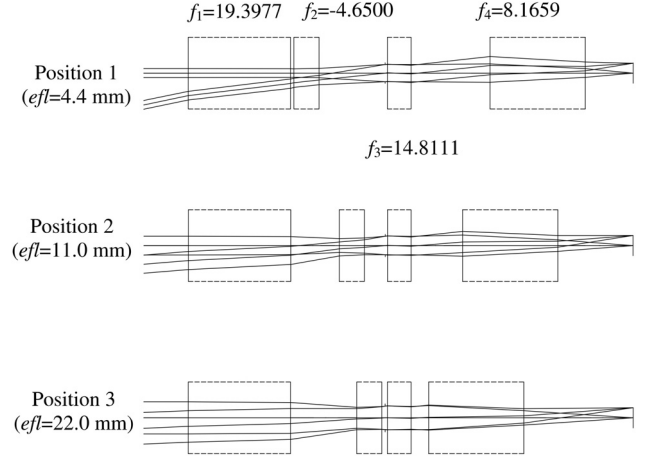


FIG. 2. Optimized zoom system consisting of the four lens modules.

first-order inputs are appropriately given to work as a zoom system. For the inner-focus zoom lens having high zoom ratio, the powers of the groups are generally composed that the first, the third, and the fourth groups have positive powers, but the second group has a negative one. The aperture stop of the system is located in front of the third module so that the system has a symmetrical configuration with respect to the stop for aberration balancing. And then we reduced the aperture and half-image size of the initial zoom system so that the third-order aberrations were dominant. We have taken the zoom system with an half-image size of 1 mm and f-numbers of F/5 at position 1 to F/7 at position 3.

In order to get an optimum zoom system, the lens module prescriptions are optimized so that the specific constraints are satisfied. The specified constraints are the overall length of system, the equal distances between the first surface and stop at all zoom positions, focal lengths of 4.4 mm at position 1 to 22.0 mm at position 3, and good imagery. The constraint on the overall length should be as short as possible to reduce the system size. The design variables of each module are the focal lengths, the front focal lengths, the back focal lengths, the conjugate points, the spaces, and the aberration coefficients.

Figure 2 shows the optimum initial zoom system obtained from this process. It has a focal length of 4.4 to 22.0 mm. Table 1 lists the design data of each module, and Table 2 gives the zooming locus at three positions. In Table 1, the values of  $W_{040}$ ,  $W_{131}$ ,  $W_{222}$ ,  $W_{220}$ , and  $W_{311}$  denote the third-order wave aberrations calculated at the edge of the field and the exit pupil in units of waves at the d-line [10]. Therefore, they correspond to the wave aberrations coefficients for spherical aberration, coma, astigmatism, Petzval curve, and distortion, respectively. In Table 2, the subscripts  $i$  denotes a zoom position for zooming.

TABLE 1. Design data (in mm) for the lens modules in the optimized lens module zoom system.

	Module I	Module II	Module III	Module IV
FL <sub>M</sub>	19.3977	-4.6500	14.8111	8.1659
FF <sub>M</sub>	-14.7547	5.0944	-14.8448	-11.6365
BF <sub>M</sub>	18.5923	-5.4960	15.6289	3.7539
MG <sub>M</sub>	0	0	0	0
ED <sub>M</sub>	1.0	1.0	1.0	1.0
Field( $\beta$ )	1.0°	1.0°	1.0°	1.0°
Thickness	9.1969	2.2552	2.1213	7.1048
W <sub>040</sub>	0.0003	-0.0150	0.0012	-0.0059
W <sub>131</sub>	0.0052	0.0097	0.0035	0.0031
W <sub>222</sub>	-0.0025	0.0002	0.0008	0.0020
W <sub>220</sub>	0.0014	0.0013	9.0e-5	3.5e-6
W <sub>311</sub>	0.0006	2.6e-6	-5.3e-6	-0.0006

TABLE 2. First-order properties and zooming locus of the zoom system consisting of four lens modules (in mm).

	Position 1	Position 2	Position 3
<i>efl</i>	4.4000	10.9948	22.0005
<i>bfl</i>	4.3086	6.7598	9.8304
<i>ffl</i>	8.7424	6.1110	-20.7254
<i>d<sub>1i</sub></i>	0.3000	4.3598	5.9478
<i>d<sub>2i</sub></i>	5.9478	1.8880	0.3000
<i>d<sub>3i</sub></i>	7.1047	4.6309	1.5854
<i>d<sub>4i</sub></i>	4.3086	6.7598	9.8304

### III. CONVERTING LENS MODULES INTO REAL LENS GROUPS

The real lens group is composed of one or several lens elements, which should be equivalent to the lens module given in Table 1. The configuration of this real lens group assumes that the aperture stop lies on the first surface of the group, and the chief ray makes an angle  $\beta$  with the optical axis at the stop [9].

The focal length ( $f$ ), the front focal length ( $ffl$ ), the back focal length ( $bfl$ ), the magnification ( $M$ ) at a given conjugate, and the third-order Seidel aberration coefficients for spherical aberration ( $S_I$ ), coma ( $S_{II}$ ), astigmatism ( $S_{III}$ ), Petzval curves ( $S_{IV}$ ), and distortion ( $S_V$ ) of this system are expressed in terms of Gaussian brackets as [8,11-12]

$$Focal\ length : f = 1 / [k_1, -d_1/n_1, k_2, \dots, -d_{l-1}/n_{l-1}, k_l], \quad (1)$$

$$Back\ focal\ length : bfl = f \cdot [k_1, -d_1/n_1, k_2, \dots, k_{l-1}, -d_{l-1}/n_{l-1}], \quad (2)$$

$$Front\ focal\ length : ffl = -f \cdot [-d_1/n_1, k_2, -d_2/n_2, \dots, -d_{l-1}/n_{l-1}, k_l], \quad (3)$$

$$Magnification : M = 1 / [-d_0, k_1, -d_1/n_1, \dots, -d_{l-1}/n_{l-1}, k_l], \quad (4)$$

$$S_I = u_0^4 \sum a_j^2 g_{2j-1} w_j, \quad (5)$$

$$S_{II} = u_0^3 \beta \sum a_j b_j g_{2j-1} w_j, \quad (6)$$

$$S_{III} = u_0^2 \beta^2 \sum b_j^2 g_{2j-1} w_j, \quad (7)$$

$$S_{IV} = H^2 \sum k_j / (n_j n_{j-1}), \quad (8)$$

$$S_V = u_0 \beta^3 \sum b_j / a_j (b_j^2 g_{2j-1} w_j + d_0^2 k_j^2 / n_j n_{j-1}), \quad (9)$$

where

$$\begin{aligned} a_j &= [-d_0, k_1, -d_1/n_1, \dots, -d_{j-1}/n_{j-1}, -c_j \cdot n_{j-1}], \\ b_j &= 1 \text{ for } j=1, \\ &= [-d_1/n_1, k_2, \dots, -d_{j-1}/n_{j-1}, -c_j \cdot n_{j-1}] \text{ for } j > 1, \\ w_j &= g_{2j}/n_j^2 - g_{2j-2}/n_{j-1}^2, \\ g_{2j} &= [-d_0, k_1, -d_1/n_1, \dots, -d_{j-1}/n_{j-1}, k_j], \\ g_{2j-1} &= [-d_0, k_1, -d_1/n_1, \dots, k_{j-1}, -d_{j-1}/n_{j-1}], \end{aligned}$$

and

$$g_{2j-2} = [-d_0, k_1, -d_1/n_1, \dots, -d_{j-2}/n_{j-2}, k_{j-1}].$$

In these equations, the subscript  $l$  denotes the final surface of the lens group,  $k_j$  ( $j=1, 2, \dots, l$ ) is the optical power of each surface,  $d_j$  ( $j=0, 1, \dots, l$ ) is the distance between surfaces, and  $u_j$  ( $j=0, 1, \dots, l$ ) is the convergence angle of the ray from the axial object point. Therefore, optical power  $k_j$  is given by  $c_j(n_j - n_{j-1})$ , where  $c_j$  and  $n_j$  are curvature and refractive index of surface, respectively. The refractive indices in the object ( $n_0$ ) and image space ( $n_l$ ) are assumed to be unity, and the square brackets denote the Gaussian brackets.

For the real lens system to be equivalent to the thick-lens module to within the limit of the first- and third-order properties, all the first-order quantities and all the third-order aberrations of the real lens should be equal to those of the lens module:

$$FL_M = 1 / [k_1, -d_1/n_1, k_2, \dots, -d_{l-1}/n_{l-1}, k_l], \quad (10)$$

$$BF_M = f \cdot [k_1, -d_1/n_1, k_2, \dots, k_{l-1}, -d_{l-1}/n_{l-1}], \quad (11)$$

$$FF_M = -f \cdot [-d_1/n_1, k_2, -d_2/n_2, \dots, -d_{l-1}/n_{l-1}, k_l], \quad (12)$$

$$MG_M = 1 / [-d_0, k_1, -d_1/n_1, \dots, -d_{l-1}/n_{l-1}, k_l], \quad (13)$$

$$W_{040} = \frac{S_I}{8}, \quad (14)$$

$$W_{131} = \frac{S_{II}}{2}, \quad (15)$$

$$W_{222} = \frac{S_{III}}{2}, \quad (16)$$

$$W_{220} = \frac{S_{IV}}{4}, \quad (17)$$

$$W_{311} = \frac{S_V}{2}, \quad (18)$$

where  $W_{040}$ ,  $W_{131}$ ,  $W_{222}$ ,  $W_{220}$ , and  $W_{311}$  are the third order wave aberrations of the lens modules given in Table 1. If Eqs. (10)~(18) are satisfied simultaneously, the real lens is equivalent to the lens module, except for chromatic aberrations. However, it is very complicated to handle all the first-order quantities and third-order aberrations at the same time.

A conversion method from lens module to the real lens has been reported [8]. However, it is very complicated to handle analytically all the first-order quantities and the third-order aberrations at the same time. In this paper, an optimization method is proposed to design a real lens equivalent to the module for each group, within the limit of paraxial optics. The design variables of the real lens are changed to obtain a lens system in which the four first-order quantities are matched to those of the lens modules. The constraints are composed of the four first-order quantities of each lens module given in Table 1, small aberrations, and overall length of each of the groups. In this process, we focused on that the zoom lens system having a compact size to realize the slim mobile camera, therefore each group has been designed with a few elements.

In a zoom system, it is desirable to have each group independently achromatized. However, that requires that two additional aberrations, axial and lateral color aberrations, be zero. In this research, general glass selections for the chromatic aberration correction are carried out instead of solving the equations. For the glass choices, flint glass is used for the negative-power elements and crown glass for the positive-power elements.

The fixed first lens group in a zoom system consists of glass block for a right-angle prism and a cemented doublet. The right-angle prism is used for reducing optical depth of the zoom system through the folding optical axis, and the cemented doublet is useful to correct the chromatic aberrations.

The second group in Table 1 has a focal length of -4.65 mm. This strong power reduces the amount of displacement of this group to have a higher zoom ratio of 5x for zooming. Also, this group is required to balance the aberrations generated by the first groups. Therefore, a singlet and a cemented doublet are needed to have a lens system equivalent to the lens modules. This confi-

guration is useful to correct the chromatic aberrations and coma. Since this group has a negative-power, the glass selection is opposed to that of the first group; *i.e.*, positive-power element has flint glass, and negative power element has crown glass.

The third group is always fixed for zooming. This makes this group free from independent color correction so that it must be as compact as possible to have a slim camera. Therefore, it is desirable to design the third group as a single element of a positive-power meniscus lens. The aspheric meniscus in this group effectively corrects the spherical aberration at all zoom positions.

The fourth group has a focal length of 8.1659 mm. This strong positive power reduces the amount of displacement of this group to have the image plane stationary for compensation. Also, this group is required to balance all the aberrations generated by the former three groups. Therefore, many lens elements are needed to have a lens system equivalent to the lens modules. The fourth lens group has an IR-cut filter. This filter cuts out the infrared ray and improves the image quality on the CCD image plane. The cemented doublet is useful to correct the chromatic aberrations for zooming, and an aspheric meniscus singlet is good for balancing the off-axis aberrations. Using the same method as described for the previous group's design, we obtained the solution for the fourth group.

#### IV. OPTIMIZED DESIGN FOR HIGH ZOOM RATIO SYSTEM

The groups separately designed in the previous section, due to the zooming locus of Table 2, are then combined to establish an actual zoom system. If a zoom system equivalent to the lens module zoom system is to be achieved, the airspaces ( $d_{ji}$ ) between groups should be set according to the zooming locus of Table 2 at each position. This procedure results in a zoom system equivalent to the lens module zoom system, as shown in Fig. 3. Table 3 shows the first-order specifications of the combined real lens zoom system. The agreement for the first-order quantities between both zoom systems is complete. However, there are color and residual aberrations that are not corrected in the first and the third groups design. If one had the freedom to change the number of elements in the actual design, one would also expect its agreement and performance to be improved.

Returning to the zoom system in Fig. 3, a plastic block is inserted to fold the ray path. It is located in front of the first lens, not inside the lens system. Its thickness is just 8 mm, a configuration which realizes a much slimmer zoom system than any other one [13]. Since the axial rays are parallel to optical axis, there are no aberrations induced by the prism block.

In the initial design, we reduced the aperture and the

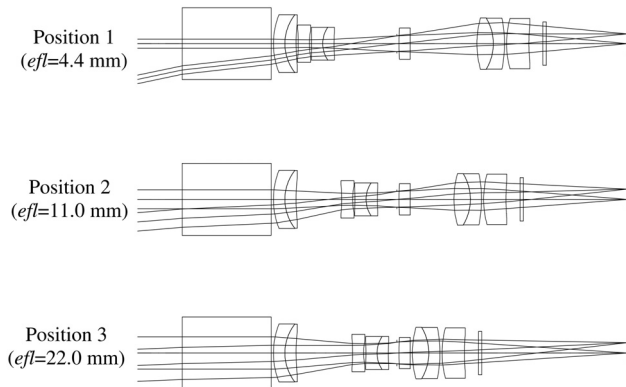


FIG. 3. Layout of an initial real lens zoom system.

TABLE 3. First-order properties and zooming locus of an initial real lens zoom system (in mm).

	Position 1	Position 2	Position 3
$efl$	4.4000	11.0000	22.0000
$bfl$	4.3086	6.7596	9.8304
$ffl$	8.7424	6.1110	-20.7250
$d_{1i}$	0.3000	4.3598	5.9478
$d_{2i}$	5.9478	1.8880	0.3000
$d_{3i}$	7.1047	4.6309	1.5854
$d_{4i}$	4.3086	6.7598	9.8304

field size so that the f-number was too large, and the image size was too small. If current specifications for a zoom camera are to be met, the aperture and the field size should be increased. The f-numbers are extended to F/3.5 at position 1 and to F/4.5 at position 3. The half image size should be 2.2 mm for 1/4-inch CCD. In an extended aperture and field system, however, higher-order aberrations that are not corrected in the previous design become significant.

In order to improve the overall performance of the zoom system with an extended aperture and field, we balance the aberrations of the starting lens given in Fig. 3 by using the lens design program. In this process, the first-order layouts are fixed. To correct the residual aberrations, we use two aspheric lenses. The aspheric surface has many design parameters, so aberrations can be well corrected [14-15].

The third group lens is a singlet and relays the refracted ray from the second group to the fourth group. Because the stop is placed in front of the third group, the axial ray heights at that group are very high at all zoom positions. Therefore, the third group generates lots of spherical aberration. Both surfaces of this lens are aspherized to balance the spherical aberrations. The fourth group is designed into a cemented lens and a singlet. To correct the distortion, it will be generally effective to use an aspheric lens at the first group.

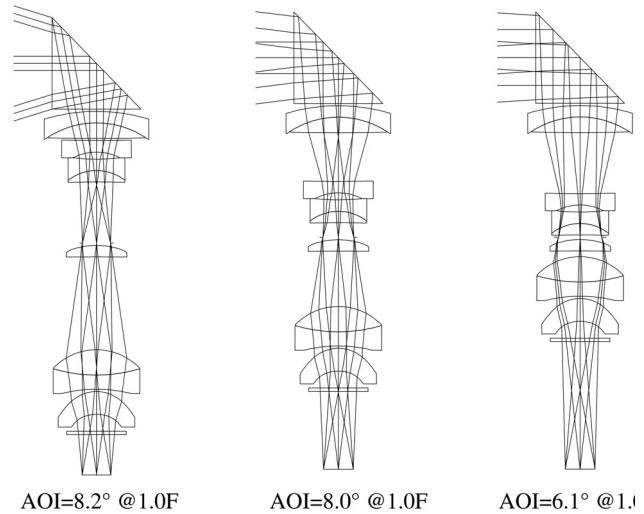


FIG. 4. Layout of an aberration-balanced zoom system using right-angle prism.

TABLE 4. Prescription data of an aberration-balanced zoom system (in mm).

Surface	Radius of C.	Thickness	Glass
Object	Infinity	Infinity	
1	Infinity	8.0000	BACD15
2	Infinity	0.2000	Air
3	16.7690	1.0000	FDS90
4	8.2009	1.3565	TAF5
5	-221.383	*0.2000	Air
6	-94.6111	1.0000	NBFD10
7	4.7184	0.6147	Air
8	-20.0973	1.0000	TAF5
9	4.2331	1.0000	FDS90
10	82.9387	*5.3450	Air
Stop	Infinity	0.2000	Air
12	Ⓐ6.8199	1.0000	FC5
13	Ⓐ123.332	*8.1257	Air
14	5.5000	2.2191	LAC8
15	-13.9696	1.2396	FDS90
16	13.1297	0.2000	Air
17	Ⓐ3.3760	2.0000	FC5
18	Ⓐ3.7120	1.4817	Air
19	Infinity	0.3000	BSC7
20	Infinity	*3.5444	
Image	Infinity	-0.0267	

(\*: air-spaces of moving groups, Ⓐ : aspheric surfaces.)

However, the distortion and the field curvature are corrected by the aspheric surfaces at the last lens of

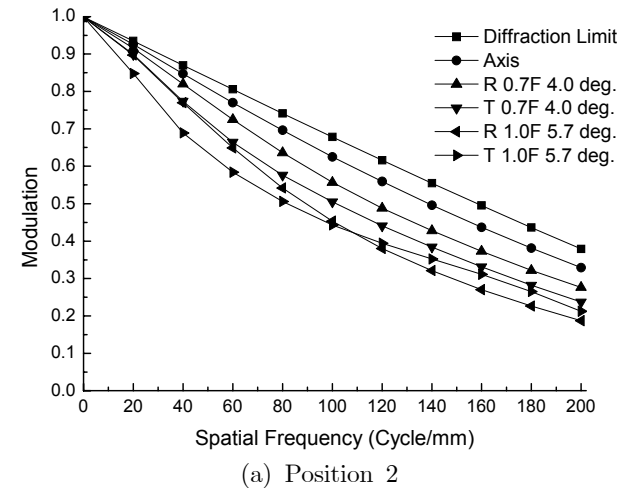
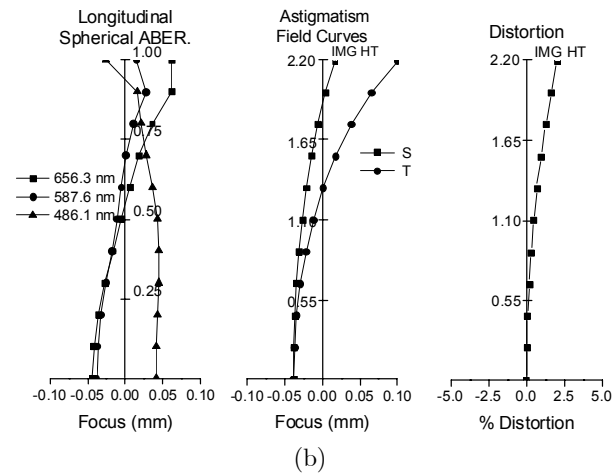
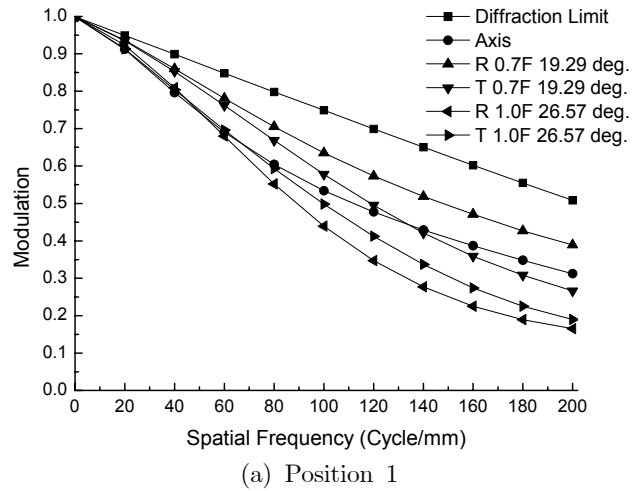
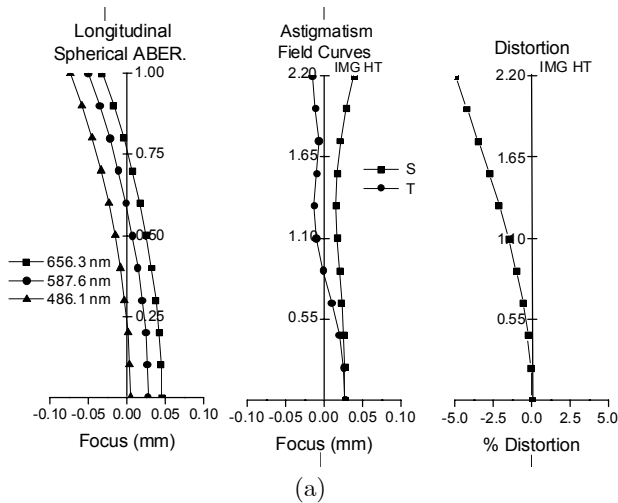


FIG. 5. Aberrations of an aberration-balanced zoom system : (a) position 1 and (b) position 3.

FIG. 6. MTF characteristics of an aberration-balanced zoom system : (a) position 1 and (b) position 3.

the fourth group in this study. It is, of course, useful to correct these aberrations because the chief ray's height in that lens is high at wide-field position.

Finally, a zoom system having good performance is obtained. The layout of the system is shown in Fig. 4. Table 4 lists the prescription data of the aberration-balanced zoom system. Figure 5 presents field aberrations, and Figure 6 shows the modulation transfer function (MTF) characteristics of the system at two extreme positions. Aberrations are significantly reduced, and the MTF at 200 lp/mm is more than 30% at all zoom positions. The relative illuminations are calculated at marginal fields for all zoom positions. In this system, the ratio of relative illuminations is more than 80% over all positions. The chief ray angles of incidence (AOI) into the image plane are shown in Fig. 4. The variation of the AOI from a wide to a narrow field is less than 2.1 degrees. That is an extremely small value, so a stable image quality for zooming can be realized. The depth of the zoom lens, even high zoom ratio of 5x, is less than 8 mm, which results in a slim and compact mobile zoom

camera. Consequently, this zoom system has enough performance to fulfill the requirements of a current mobile zoom camera.

## V. CONCLUSION

For compact zoom lens design with high zoom ratio, we set up an inner-focus zoom system consisting of four lens modules with a reduced aperture and field. The optimum initial design with a zoom ratio of 5x was derived by assigning first-order quantities and third-order wave aberrations to each module along with specific constraints.

From an optimization design procedure, a good design for the real lens of each group was quickly obtained by matching the four first-order quantities of the module and constraints. The separately designed groups were combined to establish an actual zoom system. A prism of 8 mm in thickness was inserted to fold the ray path, resulting in a slim zoom system for the mobile zoom

camera. Through balancing of the higher-order aberrations in the extended aperture and field, we improved the performance of the zoom system further. A slim zoom system with a zoom ratio of 5x, whose aperture was F/3.5 at wide field and F/4.5 at narrow field, and which had an image size of 1/4-inch on a CCD, was obtained. The zoom system developed in this work performs reasonably as a slim zoom camera system with higher zoom ratio.

### REFERENCES

1. K. Yamaji, "Design of zoom lens," in *Progress in Optics VI*, edited by E. Wolf (North-Holland, Amsterdam, The Netherlands, 1967), pp. 105-170.
2. M. S. Yeh, S. G. Shiue, and M. H. Lu, "Two-optical-component method for designing zoom system," *Opt. Eng.* **34**, 1826-1833 (1995).
3. K. Tanaka, "Paraxial analysis of mechanically compensated zoom lenses. 1: four-component types," *Appl. Opt.* **21**, 2174-2183 (1982).
4. O. Stavroudis and R. Mercado, "Canonical properties of optical design modules," *J. Opt. Soc. Am.* **65**, 509-517 (1975).
5. T. G. Kuper and M. P. Rimmer, "Lens modules in optical design," *Proc. SPIE* **892**, 140-151 (1988).
6. W. T. Welford, *Aberration of Optical Systems* (Adams Hilger Ltd., Bristol, UK, 1986), Chapter 8.
7. S. C. Park, Y. J. Jo, B. T. You, and S. H. Lee, "Optical zoom system design for compact digital camera," *J. Korean Phys. Soc.* **50**, 1243-1251 (2007).
8. S. C. Park and R. R. Shannon, "Zoom lens design using lens module," *Opt. Eng.* **35**, 1668-1676 (1996).
9. S. C. Park and Y. J. Jo, "Ultra-slim zoom lens design for a 3x mobile camera," *J. Korean Phys. Soc.* **52**, 1048-1056 (2008).
10. *CODE V Reference Manual, Version 9.70* (Optical Research Associations, Pasadena, CA, USA, 2007).
11. K. Tanaka, "Paraxial theory in optical design in terms of gaussian brackets," in *Progress in Optics XXIII*, edited by E. Wolf (North-Holland, Amsterdam, The Netherlands, 1986), pp. 63-111.
12. M. Herzberger, *Modern Geometrical Optics* (Interscience, New York, USA, 1958).
13. M. Sueyoshi, U. S. Patent, 7110186 (2006).
14. J. H. Lee, T. S. Jang, H. S. Yang, and S. W. Rhee, "Optical design of a compact imaging spectrometer for STSAT3," *J. Opt. Soc. Korea* **12**, 262-268 (2008).
15. G. I. Kweon, Y. H. Choi, and M. Laikin, "Fisheye lens for image processing applications," *J. Opt. Soc. Korea* **12**, 79-87 (2008).